# Mesenchymal stem cells aligned and stretched in self-assembling peptide hydrogels

Farzaneh Fouladgar , Forough Ghasem Zadeh Moslabeh , Yashesh Varun Kasani , Nick Rogozinski , Marc Torres , Melanie Ecker , Huaxiao Yang , Yong Yang , Neda Habibi *

*Department of Biomedical Engineering, University of North Texas, Texas, United States*

## ABSTRACT

The presented research highlights a novel approach using fmoc-protected peptide hydrogels for the encapsulation and stretching of mesenchymal stem cells (MSCs). This study utilized a custom mechanical stretching device with a PDMS chamber to stretch human MSCs encapsulated in Fmoc hydrogels. The study assessed the influence of various solvents on the self-assembly and mechanical properties of the hydrogels, and MSC viability and alignment. Particularly we focused on fluorenylmethoxycarbonyl-diphenylalanine (Fmoc-FF) prepared in dimethyl sulfoxide (DMSO), hexafluoro-2-propanol (HFP), and deionized water ($DiH_2O$).

Through molecular self-assembly of the peptide sequence into β-sheets connected by π-π aromatic stacking of F–F groups, the peptide hydrogel was found to form a stiff, hydrated gel with nanofiber morphology and a compressive modulus ranging from 174 to 277 Pa. Therefore, this hydrogel can mimic certain critical features of the extracellular matrix and collagen. Evaluations of MSCs cultured on the peptide hydrogels, including viability, morphology, and alignment assessments using various staining techniques, demonstrated that 3D-cultured MSCs in Fmoc-FF/HFP and Fmoc-FF/DMSO, followed by mechanical stretching, exhibited elongated morphology with distinct microfilament fibers compared to the control cells, which maintained a round and spherical F-actin shape. Notably, peptide gels with a concentration of 5 mM maintained 100 % MSC viability.

The findings indicate the potential and specific conditions for successful cell encapsulation and alignment within peptide hydrogels, highlighting a promising tissue engineering platform through the encapsulation of MSCs in peptide nanofibers followed by a stretching process. By enhancing our understanding of MSC-peptide hydrogel interactions, this research contributes to the development of biomaterials tailored for regenerative medicine.

## 1. Introduction

Tissue engineering aims to create functional and regenerative solutions for damaged or diseased tissues. One crucial aspect of tissue engineering is the development of hydrogels that can mimic the extracellular matrix (ECM) found in natural tissues [1]. These hydrogels should possess the inherent properties of the ECM to provide the necessary support for cell growth and proliferation while

maintaining a simplified structure [2]. Biomimetic scaffolds are expected to replicate the behavior of the ECM [3], guide stem cell growth, promote alignment [4], regulate cell behavior, and provide cues for cell differentiation [5]. Encapsulating mesenchymal stem cells (MSCs) within hydrogels and inducing their alignment and differentiation has emerged as a promising approach in tissue regeneration therapy [6]. Notably, three-dimensional (3D) encapsulation and alignment of MSCs have shown enhanced differentiation capacity compared to traditional two-dimensional (2D) cultures [7].

Biological scaffolds, including chitosan [8], polyethylene glycol polymers [9], synthetic hydro-gels [10], and natural hydrogels [11], have been utilized in tissue engineering. However, these ma-terials often lack the flexibility required to mimic the dynamic behavior of the ECM [12]. The natural ECM relies on a matrix of protein nanofibers combined with complex biomolecules to facilitate essential cellular communication [13]. To address this challenge, one promising approach involves the self-assembly of peptide-based nanofibers [14–16]. These hydrogels can be developed using small peptide molecules, which offer a simplified fabrication process while enabling the incorporation of biologically active molecules [17,18]. The resulting hydro-gels comprise nanofibrous networks that replicate the structural composition of the ECM [19]. Peptides can be synthesized using solid-liquid phase techniques, allowing for the incorporation of bioactive molecules such as RGD peptides [14] or cell anchorage amino acids in the peptide sequence, thereby promoting the development of bioactive fibers [20].

To date, most research reports have utilized peptide amphiphiles with alkyl chains to generate hydrogel scaffolds. However, the use of organic solvents in preparation of amphiphile peptides has hindered their tissue engineering applications [10]. Another challenge that has not been addressed to date is directing the self-assembly into aligned nanostructures instead of randomly organized scaffolds. This process could potentially guide MSCs growth and alignment affecting the final cell fate [2].

In this article, we present a versatile approach to developing hydrogels using Fmoc-protected dipeptides. Previous studies have shown that Fmoc-FF is capable of self-assembling into hydrogels in aqueous environments [21,22]. Furthermore, we demonstrated the use of an acoustic levitation device to manipulate and align the peptide fibers [23]. To further explore the potential of these peptide hydrogels, we employed a custom-made stretching device to align the MSC encapsulated in nanofibers gels. Our primary objectives were to investigate the effect of stretching polydimethylsiloxane (PDMS) coated with hydrogel peptides on nanofiber alignment and to assess the impact of solvent and peptide concentration on MSC viability and alignment. We employed two approaches: coating PDMS with peptide hydrogels and seeding cells on top, and combining peptide hydrogels with growth medium for cell encapsulation in microplate wells. The molecular structure of the fibers was visualized using scanning electron microscopy (SEM) and bright-field microscopy. The mechanical properties of the hydrogels were analyzed using a Microtester from CellScale. MSCs derived from bone marrow were cultured in the peptide hydrogels, and their viability, morphology, and alignment were assessed using various cell-based assays such as MTT and live/dead viability assays, as well as F-actin and DAPI staining to monitor cytoplasmic and nuclear changes.

The findings of this study demonstrate the feasibility and conditions for successful cell encapsulation and alignment within peptide hydrogels. The ability to manipulate and align MSC within nanofiber hydrogel matrix followed by stretching them provides a promising platform for tissue engineering applications. The results contribute to our understanding of the interactions between MSCs and peptide hydrogels, paving the way for the development of advanced biomaterials.

## 2. Materials and methods

Human Mesenchymal Stem Cells (Derived from Bone Marrow), catalog number: C-12974 were purchased from Millipore Sigma (USA). Cells were received as a cryopreserved vial, and was subsequently stored in liquid nitrogen. Growth mediums including MEM with no nucleosides, Catalog number: 12,561,072; L-Glutamine (200 mM) catalog number: 25,030,081; Fetal Bovine Serum certified, Catalog number: 16,000,069; Trypsin-EDTA solution, antibiotics, were purchased from Thermofisher. Cell assays such as MTT cell viability kit assay catalog number: V13154; LIVE/DEAD™ viability/cytotoxicity kit for mammalian cells, catalog number: L3224; DAPI Solution (1 mg/mL) catalog number: 62248; Alexa Fluor™ 660 Phalloidin catalog number: A22285; were all purchased from Thermofisher. Sylgard Silicone Elastomer Catalog No.50-822-180 were purchased from Fisher Scientific and was used to produce PDMS chambers. Bachem Fmoc-Phe-Phe-OH, Catalog No.50-258-618 were purchased from Fisher Scientific.

### 2.1. PDMS synthesis

The PDMS Elastomer Kit from Fisher Scientific (Catalog No.NC9285739) was employed for fabrication of PDMS substrates for seeding the MSC. The kit comprises two components: Component A, a gel in a large container, and Component B, a liquid housed in a smaller container. Component A is stored in a freezer, while Component B can be kept at room temperature. To prepare the PDMS material, a 4.5–6 g of Component A was weighed, equivalent to approximately 4–5 ml in a 15-ml falcon tube, based on the desired PDMS size. Subsequently, 0.57 g of Component B were added drop by drop to the falcon tube. The solution was thoroughly mixed using a stir rod for 5 min and then centrifuged for 10 min at 1200 rpm to eliminate any air bubbles. The resulting PDMS solution, with a stable viscosity, could be stored in the refrigerator for up to one month.

For molding, a 3D-printed mold was utilized, with metal rods strategically placed to prevent material loss during pouring. Half of the PDMS material (approximately 1.2 g) was poured into the mold and vacuumed to remove bubbles. The mold was then placed on a hot plate at 75 °C overnight for drying. After the PDMS square separated from the mold, it revealed a hollow middle section intended for the placement of a separate PDMS membrane. To fabricate the membrane, the same PDMS material was briefly centrifuged and then poured onto a glass surface. The glass, with the PDMS material, was subjected to a vacuum chamber with nitrogen gas for 10 min, followed by drying on a 60-degree Celsius hot plate for 45 min. The resulting PDMS membrane was removed using tweezers and
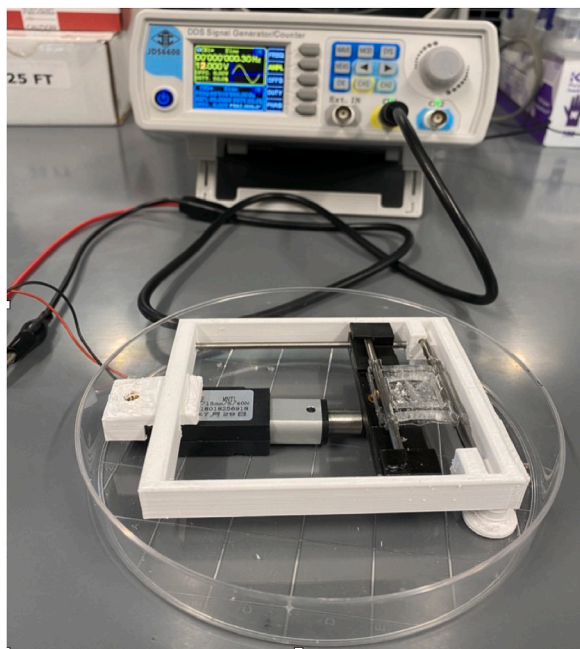
**Fig. 1.** 3D printed custom-made mechanical stretcher mounted with PDMS. Working parameters were at Frequency of 0.3 Hz, and 12 V.

attached to the PDMS square using the material itself as an adhesive. The PDMS chambers and rods were mounted on a custom-made 3D printed mechanical stretcher prepared in our lab, as shown in Fig. 1.

### 2.2. Fmoc-FF peptide hydrogels

Fmoc-FF from Bachem, Germany with a purity of 99 % was used to prepare peptide hydrogels. To dissolve the peptide, various solvents were used such as HFIP, DMSO and deionized water (pH adjusted to 10 using NaOH). Peptides were dissolved in a HFP (Hexafluoroisopropanol, 99 %) solvent with a stock concentration of 100 mg/ml, and subsequently they were diluted to a final concentration of 0.5, 2, and 5 mM using sterilized PBS, for hydrogel preparation. Peptides were also dissolved in DMSO (Dimethyl Sulfoxide, MilliporeSigma, 99 % purity) in a stock concentration of 20 mg/ml and were further diluted to 1–2 mg/ml in deionized water ($DiH_2O$) for hydrogel and nanofiber preparation. Another batch was produced which peptide stock was dissolved in water with pH 10. 2 ml of water was added to a tube containing 0.01–0.02 g of Fmoc-FF. A solution of 0.1 M NaOH, was added to the suspension to adjust pH to 10.0. The stock solution with repeated vortexing and ultrasonication was used to fully dissolve the solution until a clear solution was observed. Prior to hydrogel preparation, the pH of the solution was diluted in $DiH_2O$ and the pH was adjusted to 7 using a dropwise addition of 0.1 M HCl. Immediately after diluting the stock solution, the hydrogel formation will start. The solution was kept in a sterilized environment at 20 °C. The hydrogels were then mixed with the cell/growth medium and added to PDMS and microplate wells.

#### 2.2.1. Scanning electron microscopy and fluorescence microscopy

To determine the morphology, size, and dimension of the nanofibers and the hydrogel network, scanning electron microscopy was used. For collecting the samples, the hydrogels were diluted with $DiH_2O$ at a concentration of 1 mg/ml. Then a small portion of the solution was applied on a clean washed silicone surface and incubated for 1 h. The excess liquid was taken, followed by two rinses. The surface was then left to air-dry overnight in preparation for imaging. Images were collected with a scanning electron microscope FEI Quanta 200 ESEM.

### 2.3. Rheometry analysis

The mechanical properties of soft hydrogels were investigated using a CellScale mi-crotester rheometer (CellScale Biomaterials Testing, Microtester G2). Hydrogel samples were prepared by diluting a stock solution (100 mg/ml) of Fmoc-FF/DMSO, Fmoc-FF/HFP in Fmoc-FF/$DiH_2O$ water at a final concentrations of 5 mM. The hydrogels were molded into cylindrical shapes with a height ranging from 3001.6 to 6106.6 mm in diameter. The microtester rheometer was equipped with a beam that was 59.5 mm in length and 1.016 mm in diameter, a clamp to hold the beam in place, a 5 × 5 mm compression platen, and an anvil for the specimen to rest on during testing. The microtester rheometer was operated using the Microtester software. The hydrogel samples were mounted onto the rheometer stage by using tweezers to carefully place the hydrogel sample on the testing anvil so that it is aligned with the 1.016 mm

beam and directly underneath the $5 \times 5$ mm compression platen, ensuring minimal stress during mounting. Mechanical testing was performed by subjecting the samples to a compression magnitude that is 10 % of the specimen's original height with a constant applied force of load lasting 10 s, a hold duration of 5 s, and a recovery duration of 20 s. Data was collected for and processed through the Microtester software where the data available consists of the total duration of the test (seconds), force applied (µN), base displacement (µm), tip displacement (µm), and initial height of the sample (µm). Mechanical properties such as Stress, Strain and Elastic modulus were calculated by using 4 mm diameter sample to determine the area, the tip displacement and initial size to determine strain, then the force and area to determine stress.

### 2.4. 3D cell culture of MSC

Human MSC derived from bone marrow were cultured in a medium containing $\alpha$-MEM supplemented with 1 % L-Glutamine, Fetal Bovine Albumin 16 %, and 1 % antibiotics solu-tion. Upon obtaining a confluent cell density, cells were trypsinized with Trypsin-EDTA, and resuspended in $\alpha$-MEM medium to obtain a cell concentration of $1\text{x}10^6$-$1\text{x}10^7$/ml. Cells were stained with trypan blue and live/dead cells were analyzed with a cell counter. 1/3 of the cell/growth medium solution was utilized to encapsulate with hydrogels and the rest was passaged. Cells were seeded on a hydrogel coated microplate, as well as getting mixed with Fmoc-FF hydrogel/growth medium solutions. To prepare the Fmoc-FF hydrogels, the powder was kept at UV light for 30 min to get steril-ized. The different molar ratio of Fmoc-FF, 0.5 mM, 2 mM, and 5 mM were prepared in sterilized PBS. To encapsulate MSC, 100 µl of the Fmoc-FF were inserted into the microplate and a growth medium containing the cells were added to the wells. The mixture was pippeted to ensure homogeneity of the hydrogels. 10 ml of hydrogels in growth medium and cell suspension was seeded on a microplate. Cells seeded without hydrogels were used as a control.

### 2.5. MTT viability assay

To evaluate cell viability, the cells underwent an MTT 3-[4,5-dimethylthiazol-2-yl]-2,5 diphenyl tetrazolium bromide) assay. Initially, the cells were seeded in 96-well plates at a density of $1 \times 10^7$ cells per well and were left to adhere overnight. Following the treatment period, the medium was replaced with fresh medium containing MTT solution at a con-centration of 0.5 mg/ml, and the cells were incubated for 4 h at 37 °C. The resulting formazan crystals were dissolved in DMSO, and the absorbance was measured at 570 nm using a microplate reader [24]. All experiments were conducted in triplicate, and the data are presented as the mean $\pm$ standard deviation (SD).

### 2.6. Cell viability using LIVE-DEAD assay

The LIVE-DEAD assay was performed utilizing the LIVE/DEAD Viability/Cytotoxicity Kit, following the protocol provided by the manufacturer. In brief, the cells were incubated with a mixture of calcein-AM and ethidium homodimer-1 for 30 min at room tem-perature. Subsequently, the cells were imaged using a fluorescence microscope. The green fluorescence emitted by calcein-AM indi-cated live cells, while the red fluorescence emitted by ethidium homodimer-1 indicated dead cells. ImageJ software was employed to quantify the percentage of live and dead cells. All experiments were carried out in triplicate to ensure reliability and consistency of results [25].

### 2.7. Phalloidin assay for staining cytoplasm F-actin and DAPI assay for staining cell nucleus

To investigate the effects of the peptide compounds, the cells were treated for a duration of 72 h. When the cells reached an approximate confluency of 80 %, they were fixed using 4 % paraformaldehyde for 15 min. Subsequently, permeabilization was achieved by treating the cells with 0.1 % Triton X-100 for 10 min at room temperature. A thorough washing step with phosphate-buffered saline (PBS) followed, and then the cells were blocked with 1 % bovine serum albumin (BSA) in PBS for 1 h at room temperature.

To visualize the nuclei, the cells were stained with 4′,6-diamidino-2-phenylindole (DAPI), and for the F-actin cytoskeleton, Phal-loidin staining was employed. The staining procedure was carried out according to the manufacturer's instructions. Briefly, the cells were incu-bated with DAPI and Phalloidin for 30 min at room temperature, and subsequently washed with PBS to remove any excess staining. The stained cells were then imaged using a fluorescence microscope to observe the cellular structures. All experiments were meticulously conducted in triplicate to ensure the accuracy and reliability of the results.

## 3. Results and discussion

Self-assembling peptides such as Fmoc-FF have a unique capability to self-assemble into hydrogel and nano scaffolds. These structures have fascinating mechanical, and biomimetic properties which makes them appealing molecules to mimic ECM functions. For developing Fmoc-FF hydrogels, a stock solution of Fmoc-FF was prepared at concentrations of 100 mg/ml in HFP solvent. The stock solution was then diluted with PBS or water to a concentration of 1–2 mg/ml where immediately the fibers are formed and hydro-gelation occurs. In this study, we incorporated solvents that are compatible with cells such as DMSO and DiH$_2$O, alongside HFP to create Fmoc-FF hydrogels. This was done to examine how different solvents affect the self-assembly, mechanical properties, and bioactivity of the hydrogels. The stock solution is then diluted to prepare different gel concentrations of 0.5, 2 and 5 mM.
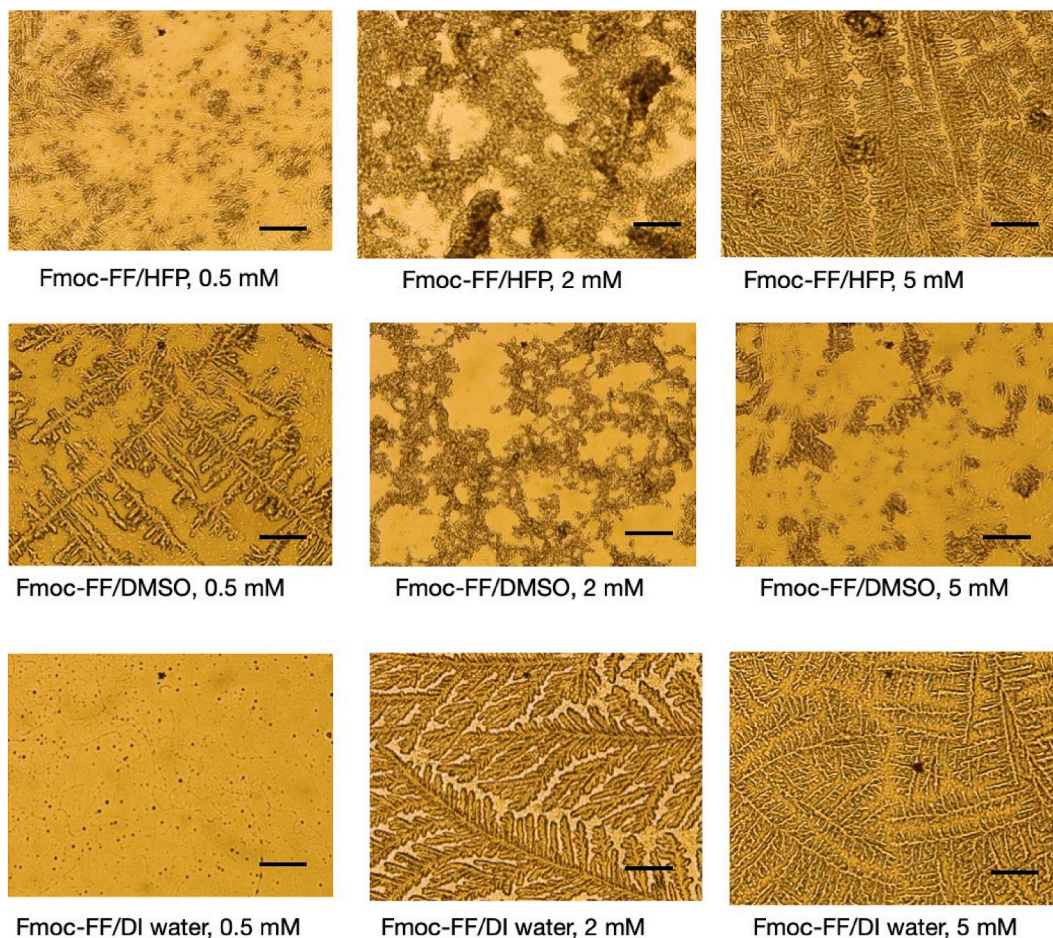
**Fig. 2.** Microscopy image of Fmoc-FF in solvents of HFP, DMSO at concentration of 0.5, 2 and 5 mM self-assembled on microplate wells. The stock of Fmoc-FF was diluted with growth medium. The scale bar is 200 μm.

First, the macroscopic hydrogel properties were observed visually (Supplement file). The visual observation of Fmoc-FF prepared in HFP, appeared to be a more rigid hydrogel compared to DMSO and DiH$_2$O water solvents. The hydrogels were formed immediately after dilution and did not leak when positioned downside in the tube. The gels formed in DMSO were more soft compared to HFP, however, rigid enough to not leak when the tube was positioned downside. The Fmoc-FF prepared in DiH$_2$O water formed a weak watery gel compared to DMSO and HFP.

We investigated the process of nanofiber formation using Fmoc-FF in various solvent systems, namely HFP, DMSO, and DiH$_2$O. To monitor the formation, we placed drops of Fmoc-FF solutions on glass slides and allowed them to dry, subsequently collecting images using a bright field microscope (Fig. 2). Our observations unveiled intriguing patterned self-assembled molecules with branched structures in the wet Fmoc-FF/HFP drops. As the concentration of the solutions increased from 0.5 mM to 5 mM, the intensity of the self-assembled structures showed a corresponding enhancement (Fig. 2). Upon analyzing the dried solutions, we observed remarkably intense self-assembled structures, with the onset of self-assembly becoming evident at a concentration of 0.5 mM and optimal formation occurring at 5 mM. Moreover, our results indicated that all Fmoc samples had the capability to form hydrogels, further underlining their potential for self-assembly. The sample of Fmoc-FF prepared in water at concentration of 0.5 mM shows a mesh of fibers which transform to branch structure in the dried sample.

The results suggest that the solubility of Fmoc-FF in the stock solution affects the final gel properties. The fmoc residue displays hydrophilic properties, while phenylalanine amino acid (FF) displays hydrophobic properties and reducing the water solubility [21]. Fmoc-FF/DiH$_2$O displayed low solubility in neutral pH. We used temperature at 37 °C and ultrasound shaking to dissolve the Fmoc-FF in water. Lower solubility of peptides in DiH2O resulted in reduced mechanical properties. Fmoc-FF was best dissolved in HFP and the gelation appeared to be more stable in this condition, however, Fmoc-FF/DMSO gels also formed comparable hydrogels to HFP.

We used SEM to image the nanofibers assembled in different solvents (Fig. 3). The dried layer of Fmoc-FF hydrogel observed with SEM displayed an entangled mesh of several fibers with bundles and interwoven structure suggesting the presence of a 3D network of nanofibers within the hydrogels. The morphology of fibers is shown in Fig. 3. The fibers were exposed as round-ribbons with a wide range of dimension and aspect ratios (Fig. 3 B). All Fmoc-FF hydrogels prepared in DMSO, HFP and DiH$_2$O contained nanofibers with
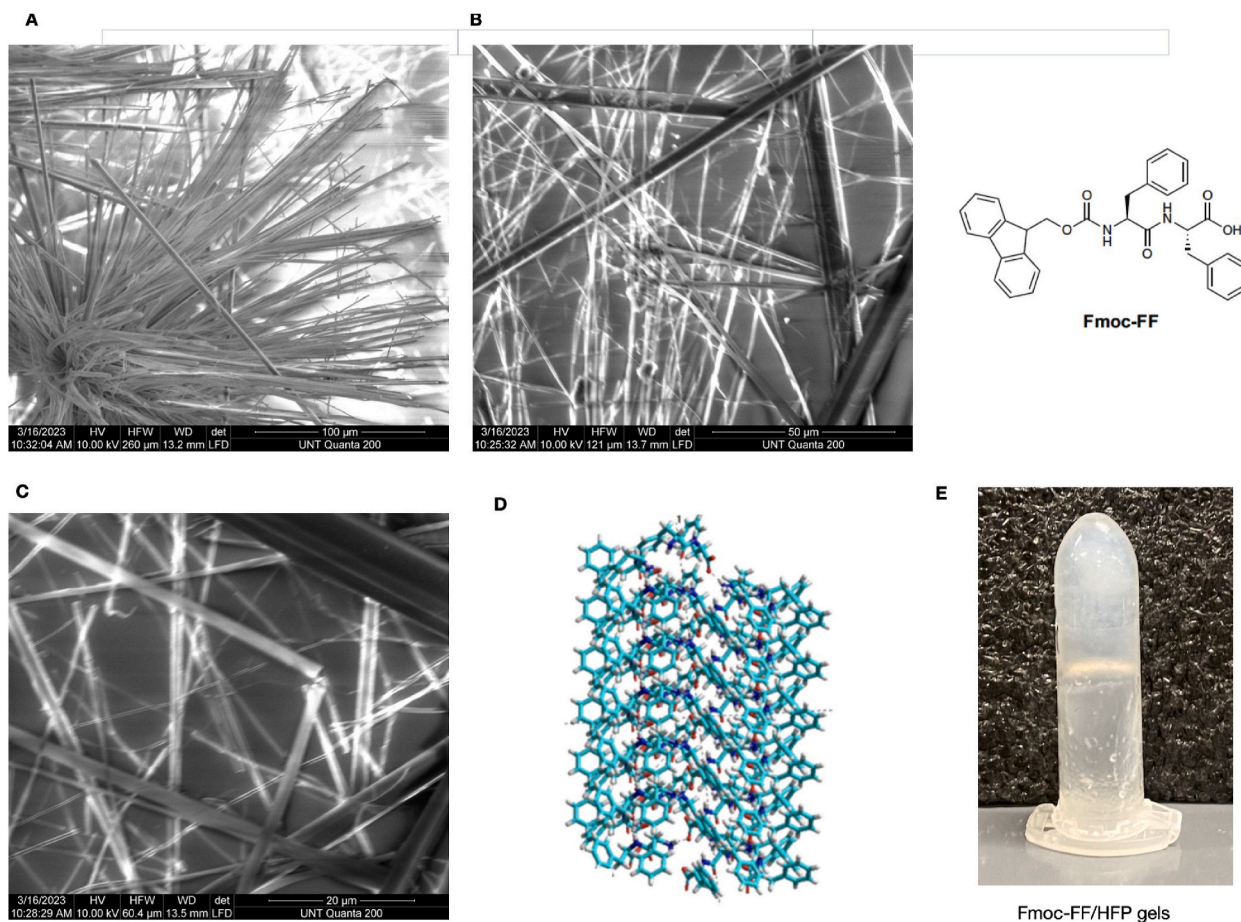
**Fig. 3.** SEM image of Fmoc-FF prepared in HFP and self-assembled on PDMS, A: The image shows bundle of interwoven nanofibers, B, C: round ribbons and small twisted nanofibers arranged perpendicular to larger fibers, D: Molecular model suggesting the β-sheets connected with hydrogen bonds and π-π aromatic stackings, E: Fmoc-FF Hydrogels prepared in microtube.

ribbon morphology. The width of larger fibers were organized parallel to each other while the smaller nanofibers were perpendicular to larger fibers (Fig. 3B and C). When the Fmoc-FF was prepared in HFP at a concentration of 5 mM, nanofibers in large bundles with repeated twist along the length was observed (Fig. 3A and B). The Fmoc-FF prepared in DMSO and DiH$_2$O exposed similar fiber morphology with the difference of less intensity of the 3D mesh network, and smaller fibers. This difference reflects the solubility of Fmoc-FF in the corresponding solvents and the molecular arrangement dominated by the hydrogelation process in various conditions.

We proposed a molecular model based on the information obtained from the morphology of Fmoc-FF that contained round ribbons and bundles (Fig. 3 D). The proposed model suggests hierarchical assembly of Fmoc-FF, which the peptide sequences of Fmoc and FF self-assembling with hydrogen intermolecular bonds that develops the β-sheet structures with antiparallel assembly. The FF molecules interact with each other through π-π aromatic stacking to lock the β-sheet. As a result of the interaction of aromatic groups and hydrogen bond and the twisted natural β-sheets, the perpendicular cylinders will shape the round ribbons. The ribbon structure is further extended into longitude assembled fibers while the Fmoc groups interact perpendicular. The fibers reach a stable structure afterwards, the width and length expansion is discontinued.

To investigate the self-assembly process of Fmoc-FF on PDMS substrates, we deposited Fmoc-FF/DMSO and Fmoc-FF/HFP solutions onto the PDMS surface. After allowing the solutions to dry, we utilized SEM imaging to analyze the results (Fig. 4A and B). The SEM images revealed distinct outcomes for the two solvent systems. In the case of Fmoc-FF dissolved in DMSO, the self-assembly led to the formation of short rods on the PDMS substrate. Conversely, Fmoc-FF dissolved in HFP yielded long fibers that intricately inter-connected, creating a mesh-like network structure. It's noteworthy that the aspect ratio of the self-assembled Fmoc-FF structures exhibited a direct correlation with both concentration and solubility in the respective solvents. Notably, prior research suggests that the formation of shorter rods in FF molecules is influenced by lower molecule concentration or reduced solubility in the solvent, indicative of the energy required for molecular cohesion [21,22].

In addition to alteration in macroscopic properties of the hydrogels, the rheometric properties of the Fmoc-FF prepared in HFP, DMSO, and water was influenced (Fig. 4C). For testing the rheometry

properties, the gels were prepared by diluting Fmoc-FF stock (HFP, DMSO, and water 100 mg/ml) in growth medium DMEM to
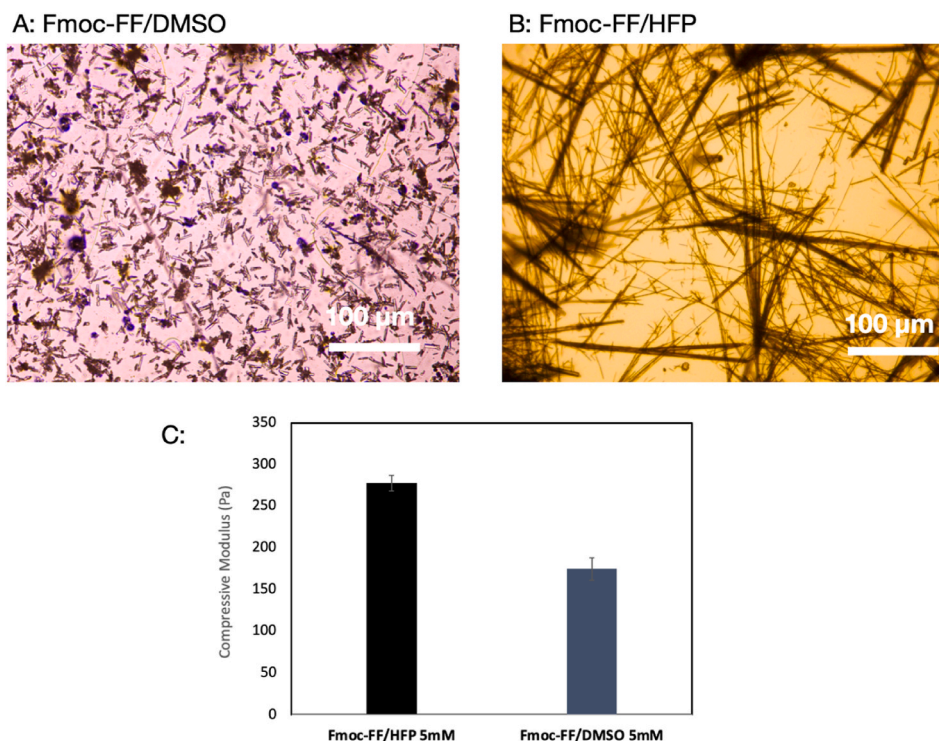
A: Fmoc-FF/DMSO

B: Fmoc-FF/HFP



**Fig. 4.** Fmoc-FF self-assembled on PDMS silicon substrates. A: The stock Fmoc-FF was prepared in DMSO and B: HFP and was diluted with deionized water; C: Compressive modulus of peptide hydrogel samples. (For interpretation of the references to colour in this figure legend, the reader is referred to the Web version of this article.)

obtain a final concentrations of 5 mM. The gels were subjected to a defined force. The resulting DMEM containing Fmoc-FF, rapidly formed a gel that reflected the stiffness of 3D-cell culture. The stress to strain curve of both hydrogel samples are presented in the supplement file. The slope of this curve recorded as the elastic modulus. The rheometric spectra obtained from CellScale Microtester displayed the E elastic modulus of Fmoc-FF/HFP, being 277.5 (Pa) and Fmoc-FF/DMSO peptides were 174.4 (Pa) indicating a solid gel. The E as an indicator of hydrogel stiffness was higher for Fmoc-FF/HFP gels compared to Fmoc-FF prepared in DMSO gels. The Fmoc-FF/DiH$_2$O had the lowest stiffness which was not measurable by the microtester. Typically, the elastic modulus of self-assembling peptides can range from a few pascals (Pa) to few kPa. This wide range is due to the versatility of these peptides in forming various structures, from soft hydrogels with low modulus values to more rigid structures with higher modulus values. In our experiment, rheometric properties were measured after 1 h to ensure the complete solidification of the hydrogels. We show that the Fmoc-FF dissolved in HFP, have higher elastic modulus compared to peptides dissolved in DMSO, and therefore suggest that mechanical properties are influenced by solvent. The gelation kinetics of peptide hydrogels are influenced by several factors, such as peptide sequence, concentration, solvent and environmental factors. Diaferia et al. suggested that a combination of Fmoc-FF/PEG-FY the gelation kinetic is increased with the presence of PEG molecules from 42 to 18 min [32]. Dudukovic et al. explored the gel transition of the aromatic dipeptide derivative molecule fluorenylmethoxycarbonyl-diphenylalanine (Fmoc-FF). The addition of water to a solution of Fmoc-FF in dimethyl sulfoxide (DMSO) results in increased attractions leading to self-assembly of Fmoc-FF molecules into a space-filling fibrous network [33,34].

When analyzing the SEM data in conjunction with the rheological data, intriguing in-sights emerge concerning the intricate relationships among molecular composition, supramolec-ular arrangement, and the hydrogel's properties. Gaining deeper insights into these relation-ships holds the potential to unlock possibilities for tailoring diverse hydrogels to specific cell types. Previous reports have highlighted that matrix stiffness can influence cell morphology and differentiation, further emphasizing the significance of exploring these connections.

The capability of the hydrogels as bioactive 3D-network was determined to support the growth of MSC derived from bone marrow. We investigated the adhesion, viability and cy-toplasm F-actin changes of MSC encapsulated in Fmoc-FF/HFP, DMSO, DiH$_2$O seeded on microplate wells. As a comparison, MSC seeded on non-modified microplate wells were utilized. First MTT and live/dead assays were used to investigate the cell's viability. Phalloidin and DAPI staining was used to monitor cytoplasm F-actin and DNA in MSC.

To encapsulate MSC into the peptide hydrogel, first the peptide was seeded on the mi-croplate wells and allowed to develop gels in aseptic conditions. Secondly, the cell suspension in growth medium was added to the wells. The cell-hydrogel structure was formed within 10 min of incubation at 37 °C. Within the first 24 h, the MSC showed a spreading condition on the scaffolds and afterwards the self-assembled structures surrounded the cells completely. The cell spreading suggest that MSC directly adhere to the scaffold.
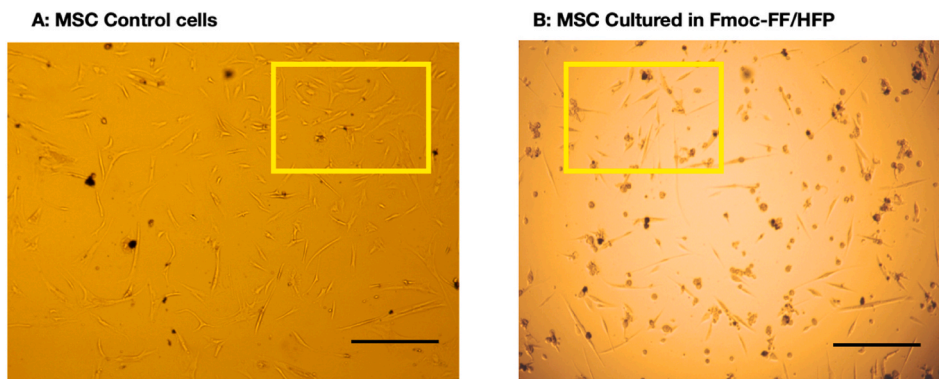
**Fig. 5.** Cell morphology of MSC cells encapsulated on peptide hydrogels Fmoc-FF/HFP, and control cells after 24 h. Scale bar 200 μm.
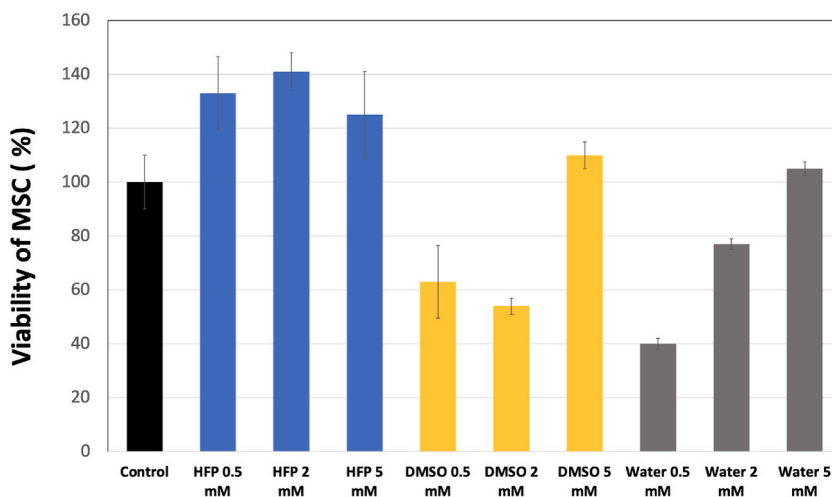


**Fig. 6.** MTT viability cell assay of MSC cells encapsulated on peptide hydrogels Fmoc-FF/HFP, Fmoc- FF/DMSO and Fmoc-FF/Water at concentrations of 0.5, 2 and 5 mM after 24 h.
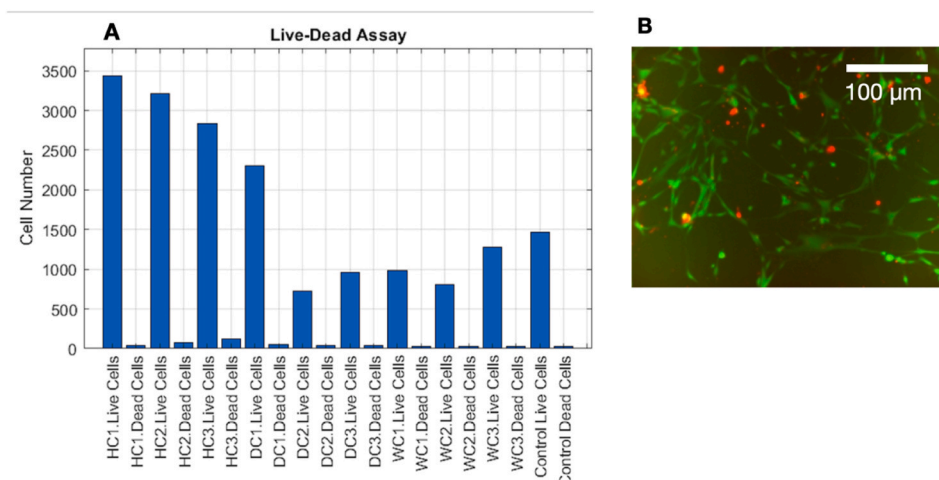


**Fig. 7.** A: LIVE-DEAD graph of live and dead cells of MSC seeded on Fmoc-FF gels prepared in HFP (HC1-3), DMSO (DC1-3) and Water (WC1-3) at concentrations of 0.5, 2, and 5 mM (C1,C2,C3). B: LIVE-DEAD staining of MSC seeded and encapsulated in Fmoc-FF/DMSO. Live cells will convert calcein AM to green fluorescent calcein, while dead cells will be stained with red fluorescent ethidium homodimer-1. (For interpretation of the references to colour in this figure legend, the reader is referred to the Web version of this article.)
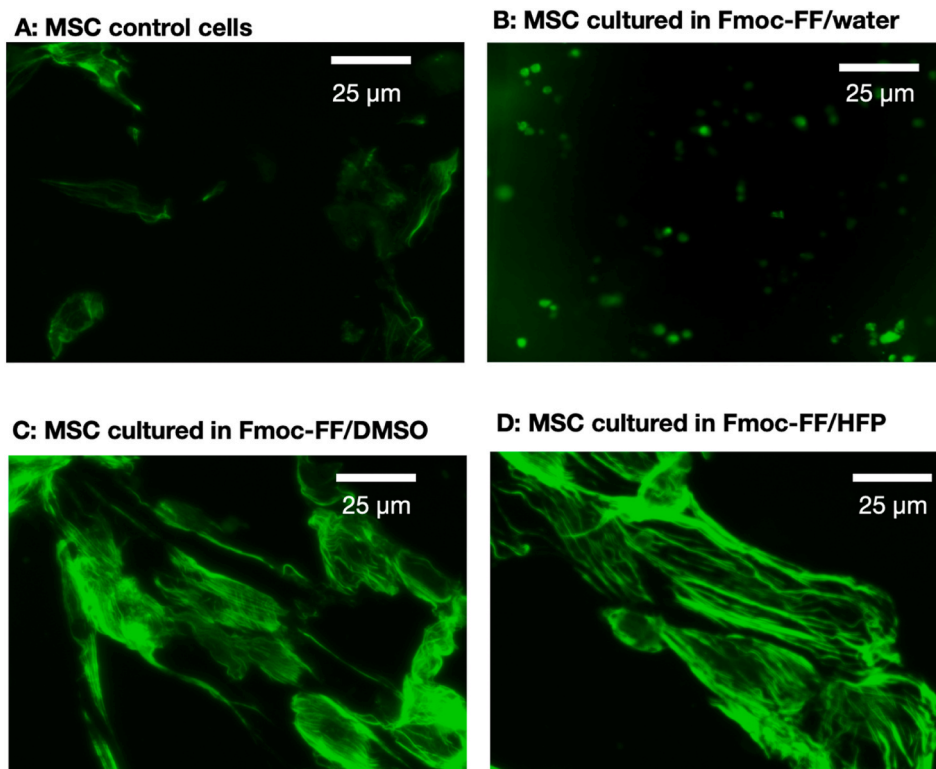
**Fig. 8.** Phalloidin (F-actin) staining of A: MSC control cells, B: MSC cultured in Fmoc-FF//water, C: MSC cultured in Fmoc-FF/DMSO, D: MSC cultured in Fmoc-FF/HFP. F-actin filaments inside the cytoplasm are stained green. (For interpretation of the references to colour in this figure legend, the reader is referred to the Web version of this article.)

Compared to the control cell group which displayed a polyhedral morphology, MSC spread and attached on peptide gels adopted a stretched spindle type morphology (Fig. 5 A, B).

According to the MTT assay (Fig. 6), at optimal concentrations, the self-assembly did not affect the MSC viability. The Fmoc-FF prepared in HFP, showed a slight increase in cell viability 120–140 %, at concentration of 0.5–5 mM compared to the control. Fmoc- FF/DMSO showed decreased viability at 0.5 (60 %) and 2 mM (50 %), while 5 mM gels had 100 % viability. Similarly, fmoc-FF/DiH$_2$O showed decreased viability at 0.5 mM (40 %), 2 mM (80 %), and 100 % viability at 5 mM gels.

We suggest that formation of stable and solid gels at concentration of 5 mM helped to encapsulate and preserve MSC viability. The cells encapsulated in DMSO and DiH$_2$O showed comparable viability to control cells indicating the bioactivity of Fmoc-FF/DMSO hydrogels. After 1 day of incubation in Fmoc-FF, the MSC were evenly attached and distributed in the hydrogels.

After 24 h of incubation, the LIVE-DEAD assay using Fmoc-FF/DMSO revealed that the majority of cells showed green staining, indicating they were alive, while only a few dead cells were observed in the entire gel (Fig. 7B). Similar to MTT results, LIVE-DEAD results showed that Fmoc-FF/HFP showed higher number of live cells compared to DMSO and water samples. DMSO and DiH$_2$O gels showed an increase in viability with higher gel concentrations (Fig. 7A).

The optimal conditions of Fmoc-FF/HFP, Fmoc-FF/DMSO at 5 mM was utilized to coat PDMS substrates with peptide hydrogels. After hydrogelation, cells were seeded on PDMS chamber and the chamber was mounted on the stretcher device. The stretcher was placed in a large Petri dish with several small dish containing Deionized water to keep the PDMS/cell culture moist at all times. The cells seeded on PDMS and encapsulated in peptide gels were stretched for 24 h with a frequency of 0.3 Hz. By staining the cells with phalloidin, the F-actin of the cells cultured on Fmoc-FF/HFP, Fmoc-FF/DMSO showed elongated morphology compared to the round and spherical F-actin shape of the control cells (Fig. 8A–D). The aligned fiber feature is suggesting defined stress fibers. In a round morphology, the F-actin filaments are generally organized in a more isotropic or symmetrical manner, which contributes to the cell's spherical shape and stability. On the other hand, elongated cell morphology indicates that the F-actin filaments are oriented in a way that promotes extension along a particular axis, leading to a more elongated or polarized cell shape. Several cellular processes can contribute to elongated cell morphology when F-actin staining shows this pattern [26,27]. Differentiation of MSC can lead to changes in the actin cytoskeleton [28], resulting in an elongated morphology associated with specialized functions [29]. The observed elongation of F-actins indicates the hydrogel effect, which promotes alignment and initiates cellular differentiation without affecting cell viability at an optimal concentrations [30,31].

## 4. Conclusion

In summary, by using a cost effective and versatile self-assembly approach, peptide gels were developed to successfully culture MSC's three-dimensionally *in vitro*. The unique molecular structure allows to encapsulate and provides a surface where cells can anchor and attach. The mechanical stretcher combined with self-assembled peptides provides a cost-effective technique for developing 3D cultures of anchorage-dependent cells. Compared to common 2D cell cultures, 3D-cultured cells better mimic the tissue microenvironment and have important implication in tissue engineering, cell therapy, and drug delivery models. All peptide samples underwent self-assembly to form hydrogels characterized by round nanofiber morphology. Notably, peptide gels prepared in HFP demonstrated the highest elastic modulus and retained their structural integrity. When it came to cell viability, Fmoc-FF/HFP gels outperformed DMSO and water samples. Additionally, MSCs encapsulated within both peptide gels in DMSO and HFP exhibited a distinct elongated spindle-like morphology, in contrast to the polyhedral shape observed in control cells. These findings collectively indicate that the utilization of peptide hydrogels to encapsulate MSCs, followed by a stretching process, represents an efficient approach to preserve the viability of MSC, assist with adhesion and potentially initiate the differentiation of these cells.

## Data availability statement

Data is included in article/supp. material/referenced in article.

## CRediT authorship contribution statement

**Farzaneh Fouladgar:** Methodology. **Forough Ghasem Zadeh Moslabeh:** Methodology. **Yashesh Varun Kasani:** Methodology. **Nick Rogozinski:** Methodology. **Marc Torres:** Methodology. **Melanie Ecker:** Validation. **Huaxiao Yang:** Investigation. **Yong Yang:** Investigation. **Neda Habibi:** Writing – review & editing, Validation, Supervision, Conceptualization.

## Declaration of competing interest

The authors declare that they have no known competing financial interests or personal relationships that could have appeared to influence the work reported in this paper.

## Acknowledgment

## Appendix A. Supplementary data

Supplementary data to this article can be found online at https://doi.org/10.1016/j.heliyon.2023.e23953.

## References

[1] P. Khayambashi, J. Iyer, S. Pillai, A. Upadhyay, Y. Zhang, S.D. Tran, Hydrogel encapsulation of mesenchy- mal stem cells and their derived exosomes for tissue engineering, Int. J. Mol. Sci. 22 (2) (2021) 684.

[2] Y. Huang, X. Li, L. Yang, Hydrogel encapsulation: taking the therapy of mesenchymal stem cells and their derived secretome to the next level, Front. Bioeng. Biotechnol. 10 (2022), 859927.

[3] C. Sobacchi, M. Erreni, D. Strina, E. Palagano, A. Villa, C. Menale, 3D bone biomimetic scaffolds for basic and translational studies with mesenchymal stem cells, Int. J. Mol. Sci. 19 (10) (2018) 3150.

[4] C. Menale, E. Campodoni, E. Palagano, S. Mantero, M. Erreni, A. Inforzato, et al., Mesenchymal stromal cell-seeded biomimetic scaffolds as a factory of soluble RANKL in Rankl-deficient osteopetrosis, Stem Cells Translational Medicine 8 (1) (2019) 22–34.

[5] Y. Tang, C. Chen, F. Liu, S. Xie, J. Qu, M. Li, et al., Structure and ingredient-based biomimetic scaffolds combining with autologous bone marrow-derived mesenchymal stem cell sheets for bone-tendon healing, Biomaterials 241 (2020), 119837.

[6] C.H. Ku, P.H. Johnson, P. Batten, P. Sarathchandra, R.C. Chambers, P.M. Taylor, et al., Collagen syn- thesis by mesenchymal stem cells and aortic valve interstitial cells in response to mechanical stretch, Cardiovasc. Res. 71 (3) (2006) 548–556.

[7] Y.J. Chen, C.H. Huang, I.C. Lee, Y.T. Lee, M.H. Chen, T.H. Young, Effects of cyclic mechanical stretching on the mRNA expression of tendon/ligament-related and osteoblast-specific genes in human mesenchymal stem cells, Connect. Tissue Res. 49 (1) (2008) 7–14.

[8] M. Boido, M. Ghibaudi, P. Gentile, E. Favaro, R. Fusaro, C. Tonda-Turo, Chitosan-based hydrogel to support the paracrine activity of mesenchymal stem cells in spinal cord injury treatment, Sci. Rep. 9 (1) (2019) 6402.

[9] C.R. Nuttelman, M.C. Tripodi, K.S. Anseth, *In vitro* osteogenic differentiation of human mesenchymal stem cells photoencapsulated in PEG hydrogels, J. Biomed. Mater. Res. 68 (4) (2004) 773–782.

[10] M. Guvendiren, J.A. Burdick, Engineering synthetic hydrogel microenvironments to instruct stem cells, Curr. Opin. Biotechnol. 24 (5) (2013) 841–846.

[11] C.N. Salinas, K.S. Anseth, Mesenchymal stem cells for craniofacial tissue regeneration: designing hydrogel delivery vehicles, J. Dent. Res. 88 (8) (2009) 681–692.

[12] M. Wagenbrenner, S. Mayer-Wagner, M. Rudert, B.M. Holzapfel, M. Weissenberger, Combinations of hydrogels and mesenchymal stromal cells (MSCs) for cartilage tissue engineering—a review of the literature, Gels 7 (4) (2021) 217.

[13] L. Martorell, A. López-Fernández, A. García-Lizarribar, R. Sabata, P. Gálvez-Martín, J. Samitier, et al., Preservation of critical quality attributes of mesenchymal stromal cells in 3D bioprinted structures by using natural hydrogel scaffolds, Biotechnol. Bioeng. 120 (9) (2023) 2717–2724.

[14] M. Zhou, A.M. Smith, A.K. Das, N.W. Hodson, R.F. Collins, R.V. Ulijn, et al., Self-assembled peptide-based hydrogels as scaffolds for anchorage-dependent cells, Biomaterials 30 (13) (2009) 2523–2530.

[15] Y.L. Wang, S.P. Lin, S.R. Nelli, F.K. Zhan, H. Cheng, T.S. Lai, et al., Self-assembled peptide-based hydro- gels as scaffolds for proliferation and multi-differentiation of mesenchymal stem cells, Macromol. Biosci. 17 (4) (2017), 1600192.

[16] Y. Wu, Z. Jia, L. Liu, Y. Zhao, H. Li, C. Wang, et al., Functional self-assembled peptide nanofibers for bone marrow mesenchymal stem cell encapsulation and regeneration in nucleus pulposus, Artif. Organs 40 (6) (2016) E112–E119.

[17] G. Onak, O. Gökmen, Z.B. Yaralı, O. Karaman, Enhanced osteogenesis of human mesenchymal stem cells by self-assembled peptide hydrogel functionalized with glutamic acid templated peptides, Journal of Tissue Engineering and Regenerative Medicine 14 (9) (2020) 1236–1249.

[18] G. Zhou, A. Tian, X. Yi, L. Fan, W. Shao, H. Wu, et al., Study on a 3D-Bioprinted tissue model of self- assembled nanopeptide hydrogels combined with adipose-derived mesenchymal stem cells, Front. Bioeng. Biotechnol. 9 (2021), 663120.

[19] R. Li, J. Xu, D.S.H. Wong, J. Li, P. Zhao, L. Bian, Self-assembled N-cadherin mimetic peptide hydrogels promote the chondrogenesis of mesenchymal stem cells through inhibition of canonical Wnt/$\beta$-catenin signaling, Biomaterials 145 (2017) 33–43.

[20] A. Huang, D. Liu, X. Qi, Z. Yue, H. Cao, K. Zhang, et al., Self-assembled GFFYK peptide hydrogel enhances the therapeutic efficacy of mesenchymal stem cells in a mouse hindlimb ischemia model, Acta Biomater. 85 (2019) 94–105.

[21] S. Yazdani, S.M. Ghoreishi, N. Habibi, Effects of Co-solvents on loading and release properties of self-assembled di-peptide building blocks, towards drug delivery applications, Protein Pept. Lett. 29 (1) (2022) 80–88.

[22] N. Habibi, N. Kamaly, A. Memic, H. Shafiee, Self-assembled peptide-based nanostructures: smart nano- materials toward targeted drug delivery, Nano Today 11 (1) (2016) 41–60.

[23] F.G.Z. Moslabeh, F. Fouladgar, A. Jafari, N. Habibi, Substrate-free self-assembly of peptides nano-particles through acoustic levitation, Colloids Surf. A Physicochem. Eng. Asp. 657 (2023), 130439.

[24] P. Kumar, A. Nagarajan, P.D. Uchil, Analysis of cell viability by the MTT assay, Cold Spring Harb. Protoc. 2018 (6) (2018) pdb-prot095505.

[25] B.A. Pfeffer, S.J. Fliesler, Streamlined duplex live-dead microplate assay for cultured cells, Exp. Eye Res. 161 (2017) 17–29.

[26] L. Zhang, N. Tran, H.Q. Chen, X. Wang, Cyclic stretching promotes collagen synthesis and affects F-actin distribution in rat mesenchymal stem cells, Bio Med. Mater. Eng. 18 (4–5) (2008) 205–210.

[27] S. Ghazanfari, M. Tafazzoli-Shadpour, M.A. Shokrgozar, Effects of cyclic stretch on proliferation of mesenchymal stem cells and their differentiation to smooth muscle cells, Biochem. Biophys. Res. Commun. 388 (3) (2009) 601–605.

[28] B. Xu, Y. Ju, G. Song, Mechanical stretch-induced f-actin reorganization and tenogenic differentiation of human mesenchymal stem cells, J. Biol. Res. 18 (2012) 218.

[29] M.C. Qi, J. Hu, S.J. Zou, L.C. Han, E. Luo, The changes of cytoskeleton F-actin in rat bone marrow mesenchymal stem cells and calvarial osteoblasts under mechanical strain, Hua xi kou Qiang yi xue za zhi= Huaxi Kouqiang Yixue Zazhi= West China Journal of Stomatology 23 (2) (2005) 110–112.

[30] Zy Wang, S.H. Teoh, N.B. Johana, M.S.K. Chong, E.Y. Teo, Mh Hong, et al., Enhancing mesenchymal stem cell response using uniaxially stretched poly ($\varepsilon$-caprolactone) film micropatterns for vascular tissue engineering application, J. Mater. Chem. B 2 (35) (2014) 5898–5909.

[31] J.M. Maloney, D. Nikova, F. Lautenschläger, E. Clarke, R. Langer, J. Guck, et al., Mesenchymal stem cell mechanics from the attached to the suspended state, Biophys. J. 99 (8) (2010) 2479–2487.

[32] C. Diaferia, M. Ghosh, T. Sibillano, E. Gallo, M. Stornaiuolo, C. Giannini, G. Morelli, L. Adler-Abramovich, A. Accardo, Fmoc-FF and hexapeptide-based multicomponent hydrogels as scaffold materials, Soft Matter 15 (2019) 487–496.

[33] N.A. Dudukovic, C.F. Zukoskib, Gelation of Fmoc-diphenylalanine is a first order phase transition, Soft Matter 11 (2015) 7663–7673.

[34] A.M. Kloxin, C.J. Kloxin, C.N. Bowman, K.S. Anseth, Mechanical properties of cellularly responsive hydrogels and their experimental determination, Adv. Mater. 22 (2010) 3484–3494.